

Hubble Space Telescope Imaging of the Globular Cluster System around NGC 5846¹

Duncan A. Forbes

Lick Observatory, University of California, Santa Cruz, CA 95064

and

School of Physics and Space Research, University of Birmingham, Edgbaston, Birmingham B15 2TT, United Kingdom

Electronic mail: forbes@lick.ucsc.edu

Jean P. Brodie

Lick Observatory, University of California, Santa Cruz, CA 95064

Electronic mail: brodie@lick.ucsc.edu

John Huchra

Harvard-Smithsonian Center for Astrophysics, 60 Garden Street, Cambridge, Massachusetts 02138

Electronic mail: huchra@cfa.harvard.edu

ABSTRACT

Bimodal globular cluster metallicity distributions have now been seen in a handful of large ellipticals. Here we report the discovery of a bimodal distribution in the dominant group elliptical NGC 5846, using the *Hubble Space Telescope's* Wide Field and Planetary Camera 2 (WFPC2). The two peaks are located at $V-I = 0.96$ and 1.17 , which roughly correspond to metallicities of $[Fe/H] = -1.2$ and -0.2 respectively. The luminosity functions of the blue and red subpopulations appear to be the same,

¹Based on observations with the NASA/ESA *Hubble Space Telescope*, obtained at the Space Telescope Science Institute, which is operated by AURA, Inc., under NASA contract NAS 5-26555

indicating that luminosity does not correlate with metallicity within an individual galaxy's globular cluster system.

Our WFPC2 data cover three pointings allowing us to examine the spatial distribution of globular clusters out to 30 kpc (or 2.5 galaxy effective radii). We find a power law surface density with a very flat slope, and a tendency for globular clusters to align close to the galaxy minor axis. An extrapolation of the surface density profile, out to 50 kpc, gives a specific frequency $S_N = 4.3 \pm 1.1$. Thus NGC 5846 has a much lower specific frequency than other dominant ellipticals in clusters but is similar to those in groups. The central galaxy regions reveal some filamentary dust features, presumably from a past merger or accretion of a gas-rich galaxy. This dust reaches to the very nucleus and so provides an obvious source of fuel for the radio core. We have searched for proto-globular clusters that may have resulted from the merger/accretion and find none. Finally, we briefly discuss the implications of our results for globular cluster formation mechanisms.

1. Introduction

One of the most interesting recent developments in globular cluster (GC) studies is the discovery that at least some elliptical galaxies have a bimodal GC metallicity distribution. A bimodal distribution is also seen in the Milky Way GC system. These bimodal, and sometimes possibly trimodal, distributions are more metal-rich in the mean than those of the Milky Way but the same general conclusion can be drawn from their existence; galaxies with multimodal metallicity distributions have not undergone a simple monolithic collapse but have experienced episodic star formation. To date, the best examples of multimodal GC metallicity distributions are cD galaxies with extremely rich GC systems (i.e. with specific frequency $S_N \sim 15$) such as M87 in Virgo (McLaughlin, Harris & Hanes 1994), NGC 1399 in Fornax (Bridges, Hanes & Harris 1991) and NGC 3311 in Hydra (McLaughlin *et al.* 1995). Two galaxies with ‘normal’ specific frequencies have also revealed bimodal distributions i.e., NGC 4472 with $S_N = 5.6$ (Geisler *et al.* 1996) and NGC 3923 with $S_N = 6.4$ (Zepf, Ashman & Geisler 1995). Thus the formation mechanism responsible for two distinct GC populations must be able to explain both the populous GC systems in cD galaxies, and the ‘normal’ richness GC systems in ellipticals.

An interesting galaxy in this regard is NGC 5846. Although it dominates a small, compact group of galaxies it has an average or slightly below average specific frequency. Detection of a bimodal GC color distribution in this galaxy would add a further constraint to GC formation mechanisms. The galaxy is not a cD but a giant E0 elliptical, with an effective radius of 11.6 kpc (Bender, Burstein & Faber 1992) and an absolute magnitude of $M_V =$

-22.6 (Faber *et al.* 1989), assuming a distance modulus $(m-M) = 32.3$ from Forbes, Brodie & Huchra (1996; hereafter Paper I). This would place NGC 5846 some 13 Mpc more distant than the Virgo cluster. Harris & van den Bergh (1981) estimated the total GC count, from a photographic study, to be 2200 ± 1300 . For $M_V = -22.6$ this corresponds to $S_N = 2.0 \pm 1.2$. (Note that Harris & van den Bergh used $M_V = -21.7$ and hence derived $S_N = 4.5 \pm 2.6$.)

The inner region of NGC 5846 contains some dust and a compact radio core with a possible extended component (Mollenhoff, Hummel & Bender 1992). The X-ray emission from hot gas extends ~ 100 kpc from the center of the galaxy, encompassing two other early-type galaxies in the group (Biermann, Kronberg & Schumutzler 1989). Biermann *et al.* calculated the hot gas mass to be $\sim 10^{11}M_\odot$, and the total virial mass to be almost $10^{13}M_\odot$. Recent ROSAT mapping reveals that the soft X-ray emission is spatially coincident with the $H\alpha$ emission and dust morphology (Goudfrooij & Trinchieri 1996). The galaxy shows many characteristics similar to those of M87, which lies at the center of the Virgo cluster. Both are luminous galaxies ($M_V = -22.5$ for M87) which dominate the local potential and lie at the center of an extensive X-ray envelope. The virial mass and cooling flow infall rate are also similar for the two galaxies. The central velocity dispersion is 361 km s^{-1} for M87 and 278 km s^{-1} for NGC 5846 (Faber *et al.* 1989). They differ greatly in one important regard, namely GC specific frequency ($S_N = 14 \pm 0.5$ for M87). It has been speculated that some of M87’s GCs were formed as a result of its location at the center of a large gravitational potential, either from the cooling flow (Fabian, Nulsen &

Canizares 1984), or by accretion from neighboring galaxies (e.g. Forte *et al.* 1982) or from the field (West *et al.* 1996). Knowledge of the GC system properties of NGC 5846, particularly in comparison with giant ellipticals in different environments, may provide important clues about globular cluster and galaxy formation histories.

In paper I we presented the V band WFPC2 data for NGC 5846. The GC luminosity function (GCLF) was found to be the same in each of three separate pointings, ranging from ~ 3 to 30 kpc from the galaxy center. While taking into account incompleteness, photometric errors and background contamination we fit the combined GCLF using the maximum likelihood technique of Secker & Harris (1993). This gave a turnover magnitude of $m_V^0 = 25.05 \pm 0.10$ and a dispersion of $\sigma = 1.34 \pm 0.06$. Here we include the WFPC2 I band data and discuss the color and spatial distributions of the GC system in NGC 5846.

2. Observations and Data Reduction

Details of the observations and data reduction are described in Paper I. Briefly, we obtained WFPC2 images of NGC 5846 at three pointings, in two filters. The pointings are located ~ 1.5 arcmin north of the nucleus, ~ 2.5 arcmin south and one with the galaxy centered in the PC CCD. For each filter, we have a pair of images giving a total of 2400 seconds in F555W and 2300 seconds in F814W. Objects were detected using DAOPHOT (Stetson 1987) with a S/N threshold of 4 per pixel. Aperture magnitudes (in a 2 pixel radius) were converted to total Johnson V and Cousins I mags. A Galactic extinction correction ($A_V = 0.11$ and $A_I = 0.05$) was also applied. The DAOPHOT-selected object list was checked for matches to

hotpixels and all sources with FWHM greater than 3 pixels were removed. Contamination in the final object list is expected to be less than 5%. Completeness tests for the V band data indicate a 50% incompleteness at $V = 25.95$. Photometric errors at this magnitude are 0.16. In this paper we include GCs in the central PC which are located at galactocentric distances of greater than $7''$ (1 kpc) i.e., beyond the strongest dust lanes. Globular clusters located interior to this radius are discussed separately in section 4.1.

3. Results

3.1. The Galaxy

We have subtracted a smooth model of the galaxy from the PC CCD image of the central pointing. A grey scale of the residuals is shown in Fig. 1 (Plate **) which reveals several GCs along with filamentary dust features. The DAOPHOT selected GCs, beyond $7''$ of the galaxy center, are indicated. In Fig. 2 we give radial profiles of some parameters from the I band galaxy model (which is less affected by dust than the V band). The surface brightness profiles show that the V–I color is roughly constant between 0.1 and 3 kpc. Both V and I profiles show a change in slope at about 0.3 kpc or $2.3''$. The ellipticity profile confirms that the galaxy is E0–1 in the central regions. The position angle changes from 70° to $\sim 100^\circ$ near the nucleus, and 4th cosine term (see for example Forbes & Thomson 1992) becomes more boxy which indicates extra light at 45° to the major axis.

3.2. The Globular Clusters

The color–magnitude diagram for our full sample of 837 GCs, from all three pointings, is shown in Fig. 3. The GCs range from $V \sim$

21 to $V \sim 26$. There is a hint of bimodality, best seen between $24 < V < 25$, otherwise the average color is relatively constant with magnitude.

The mean color, weighted by photometric error, is $V-I = 1.15$ with a rms scatter of $\pm 0.2 \pm$ or in terms of an error on the mean of ± 0.01 . In the subsequent analysis, we have confined the sample to have colors within 3σ of the mean. This excludes 63 objects with extreme blue and red colors. These objects appear to be distributed randomly throughout the three pointings, in particular they are *not* centrally located. The objects with the extreme colors tend to be the faintest sources, suggesting that photometric errors have affected their colors. Histograms for the color-selected subsample are shown in Fig. 4. Here a color histogram is given for each of the pointings and for all three pointings combined. A clear bimodal color distribution is seen in the north and south pointings (and is reflected in the combined histogram), with peaks located at $V-I = 0.96$ and 1.17 . The central pointing reveals the red peak, with a hint of some additional blue GCs.

Bearing in mind that the conversion of color into metallicity is uncertain, we use the relation of Couture *et al.* (1990) to derive $[\text{Fe}/\text{H}]$ from $V-I$. The rms error in this relation (~ 0.25 dex) dominates over the error associated with measuring the mean GC color. Their relation gives a mean metallicity for the GC system of $[\text{Fe}/\text{H}] = -0.3 \pm 0.25$. In Fig. 5 we show GC metallicity as a function of galactocentric distance expressed in kpc. A weighted fit to $[\text{Fe}/\text{H}]$ versus log of the distance in arcsec gives a linear slope of -0.13 ± 0.03 over the radial range of 1 to 30 kpc. This indicates that the gradient is significant at the 4σ level.

The surface density distribution of GCs around NGC 5846 has been calculated using two different methods. The first, applied to the central pointing, is to make use of the fact that out to some radius the WFPC2 gives almost complete 180° coverage for one hemisphere of the galaxy. This hemisphere is $\pm 90^\circ$ about the WFPC2 V3 axis. Thus we have counted up the GCs in six half-annuli from 1 to 13 kpc. The number in each half-annulus is doubled to give the full 360° coverage, and divided by the area of the annulus. For the two offset pointings, the orientation of the WFPC2 field-of-view with respect to the galaxy is much more complicated. In the second method, we simply count up the number of GCs per CCD and divide by the CCD area. As the GCs are not uniformly distributed across the CCD, we use the median galactocentric distance as a weighted distance. Surface densities from the two methods are given in Fig. 6 which shows a smooth transition between the two methods. A fit to the surface density distribution using

$$\rho = \rho_o r^\alpha$$

gives $\alpha = -0.7 \pm 0.1$ and $\rho_o = 4.8 \pm 0.5$ (assuming negligible background contamination).

We can use the surface density profile to estimate the total number of GCs around NGC 5846. First we must correct for the faint undetected GCs. From our GCLF fitting in Paper I we estimate that $\sim 25\%$ of GCs were not detected. Thus the normalization constant ρ_o should be increased to 6.0. The uncertainty in calculating the total number of GCs is dominated by the choice of the outer radius. The GC counts of Harris & van den Bergh (1981) reached the background level at

$\sim 6'$ (50 kpc). Integrating the profile out to this radius gives a total of 4670 GCs and a corresponding specific frequency of $S_N = 4.3 \pm 1.1$. Integrating to 60 kpc would increase the number of GCs by 1270. In addition to a global S_N , we can also estimate S_N as a function of radius from our central pointing. Using the integrated galaxy V magnitude at various radii, from the catalog of Longo & de Vaucouleurs (1983), we can calculate the ‘local’ S_N value from our GC counts. The S_N values as a function of galactocentric distance are shown in Fig. 7.

The radial distribution of V magnitude is shown in Fig. 8. The mean magnitude shows little change with distance from the galaxy center. The azimuthal distribution of GC counts is shown in Fig. 9. Here we have restricted GCs to lie within 13 kpc and between position angles of -25° and 155° in order to obtain complete coverage in one hemisphere. We find a slight enhancement of GCs around 20° and a deficit around 100° .

4. Discussion

4.1. Central Regions

The galaxy central regions reveal a number of GCs and filamentary dust. The central dust indicates a past merger or accretion of a gas-rich galaxy and appears to reach right into the nucleus. Given the short dynamical timescale, for galactocentric distances of < 0.5 kpc, the dust (and gas) provides an obvious source of fuel for the compact radio core (Mollenhoff *et al.* 1992). A number of proto-globular clusters have been detected in currently merging galaxies (e.g. Holtzman *et al.* 1992; Whitmore *et al.* 1993; Whitmore & Schweizer 1995; Holtzman *et al.* 1996), as predicted by the Ashman & Zepf (1992)

merger model. These objects, initially blue and very bright, will fade and redden with time. Thus depending on the epoch of formation of GCs, we may expect to see a population of very blue or very red GCs. A search for proto-globular clusters in NGC 5846 is problematic due to the dust. As mentioned in section 2, we excluded regions within $7''$ (1 kpc) of the galaxy nucleus from our object list. We have decided to visually inspect the inner $7''$ in *both* the V and I images for GCs. Although not objective, the eye is good at recognizing the brighter sources. We find 9 objects, some on the edges of dust lanes. The V magnitudes and colors range from $23 < V < 24$ and $0.9 < V-I < 1.7$. The mean color is $V-I = 1.15$ which is the same as the mean for the full sample. Thus we find *no* evidence for a centrally concentrated population of GCs with extreme colors. Furthermore, if we assume that all objects are intrinsically redder than $V-I = 0.9$, then we can place a lower limit on their age from stellar population models. Using Bruzual & Charlot (1996), a cluster with $V-I > 0.9$ and solar metallicity is at least 1 Gyr old. This suggests that *if* these central GCs formed from a gas-rich merger, then it occurred over 1 Gyr ago. The spectroscopic study of NGC 5846 by Fisher, Franx & Illingworth (1995) would tend to support this idea, as they found no evidence for a young stellar population and concluded that the stars were uniformly old (~ 15 Gyr).

The galaxy surface brightness profiles (Fig. 2) do *not* continue to rise with the same slope in the very inner regions i.e., the profiles flatten off. These so-called ‘shallow cusps’ have been seen in *HST* observations of several galaxies (e.g. Forbes *et al.* 1995; Lauer *et al.* 1995; Carollo *et al.* 1996). If we fit the V band profile with the dual power-law of Lauer

et al. we derive an inner slope of -0.2 . For $M_V = -22.6$, this value lies on the correlation of inner slope versus absolute V magnitude (Forbes *et al.* 1995). Although the origin for this correlation is still subject to debate, it is not the result of dust obscuration but rather some fundamental scaling relation in galaxies. NGC 5846 obeys this scaling relation.

4.2. Color Distribution

The distribution of GC V–I color reveals a bimodal structure, with peaks around V–I = 0.96 and 1.17 (Fig. 4). A KS test confirms that the blue subpopulation is statistically significant and a reduced χ^2 goodness-of-fit indicates that two Gaussians (with six free parameters) are a better fit to the color distribution than one Gaussian (with three free parameters). Assuming the color–metallicity relation of Couture *et al.* (1990), these colors correspond to metallicities of $[\text{Fe}/\text{H}] = -1.2$ and -0.2 respectively. In order to study the blue and red subpopulations separately, we have defined a blue sample of 232 GCs with colors of $0.84 < \text{V} - \text{I} \leq 1.06$ and a red sample of 361 with $1.06 < \text{V} - \text{I} \leq 1.28$. The ratio of the red to blue samples changes from 1.70 for the central pointing to 1.34 for the north and 1.54 for the south pointings. This tends to suggest that the red subpopulation is more centrally concentrated than the blue population. We measure a small radial metallicity gradient, $\Delta[\text{Fe}/\text{H}]/\Delta\log R$ (arcsec) = -0.13 ± 0.03 . In the case of NGC 4472, a metallicity gradient of -0.4 in $\Delta[\text{Fe}/\text{H}]/\Delta\log R$ (arcsec) was seen by Geisler *et al.* (1996) using Washington photometry. They concluded that the gradient was probably due to the changing proportions of the two subpopulations rather than a smoothly varying radial gradient.

Next we examine whether or not the blue

(metal-poor) and red (metal-rich) samples have different luminosity functions. The dependence of GC luminosity on metallicity pertains to various aspects of GC formation and evolution i.e. self-enrichment, the extent to which massive GCs can retain heavy elements from the first generation of stars and the ability of proto-globular clusters to sweep up enriched material during passage near the galaxy center. There is, at present, no generally accepted model of GC formation and no firm physical basis for assuming that the GCLF is universal. It is generally assumed that the mass-to-light ratio of all GCs is the same and, therefore, that the mass and luminosity functions have the same form. For Milky Way and M31 GCs there is no luminosity–metallicity dependence (Huchra, Brodie & Kent 1991), but this question remains largely unaddressed for galaxies beyond the Local Group. Bimodal color, and by inference metallicity, distributions have been reported in a number of galaxies (see the list of Kissler-Patig 1996) but a comparison of the luminosity functions of the two subpopulations has so far been attempted only for M87. Whitmore *et al.* (1995) and Elson & Santiago (1996) each find evidence for bimodal color distributions in their WFPC2 images of the M87 GC system. They also claim that the red subpopulation is on average fainter than the blue subpopulation by 0.13 (Whitmore *et al.*) and 0.3 (Elson & Santiago).

In Fig. 10 we show the V band GCLF for the blue and red subpopulations of NGC 5846 compared to a Gaussian fit to the full sample in Paper I. Although there is considerable scatter in each magnitude bin, both the blue and red subpopulations appear to be consistent with the same Gaussian (i.e. fixed

turnover magnitude and dispersion). This is confirmed by a K–S test which indicates that the two subpopulations are *not* statistically different. In order to test our ability to detect an offset in the two GCLFs we have progressively faded the red sample. These tests indicate that the two samples become statistically different only for offsets greater than 0.3 mag, i.e. we can not confirm offsets of less than 0.3 magnitudes. Elson & Santiago (1996) do not quote the statistical significance of their 0.3 magnitude offset. For NGC 5846, we conclude that the blue and red GC populations have similar luminosity functions. There is no strong evidence for a luminosity–metallicity relation for GCs within a single galaxy’s GC system. This does not, however, rule out the possibility of a GC luminosity–metallicity relation *between* galaxies. Indeed such a relationship may allow us to understand the connection between GCLF turnover magnitude, GC metallicity (Ashman, Conti & Zepf 1995) and parent galaxy total luminosity (Secker & Harris 1993).

4.3. Spatial Distribution

The radial variations of GC properties may constrain theories of GC formation and destruction. In Paper I we showed that the GCLF did not vary with galactocentric radius. Excluding the PC CCDs (which have a slightly brighter detection limit), we now show in Fig. 8 that the mean GC magnitude is roughly constant, out to 30 kpc. If the mass-to-light ratio is constant, this implies that the mean mass of GCs does not vary with distance from the galaxy center. A similar result was found by Forbes *et al.* (1996) for a sample of 14 nearby ellipticals. Destruction processes, such as dynamical friction, appear to be insignificant over the radial range

probed by our data. This result, and Forbes *et al.* (1996), appear to rule out the model of Murali & Weinberg (1996) on GC evolution.

Fig. 5 shows that the metallicity (as derived from V–I colors) has a slight dependence on galactocentric radius. This gradient is generally smaller than that measured in other giant elliptical and cD galaxies, but these results seem to be consistent with the observed trend of metallicity with specific frequency (see Forbes, Grillmair & Brodie 1996). Gradients are expected in both the Ashman & Zepf (1992) merger and dissipational collapse pictures. However, projection effects tend to reduce such gradients (e.g. Secker 1996). The Searle & Zinn (1978) picture of coalescing subunits, on the other hand, predicts no radial metallicity gradient.

The surface density of GCs in log space is shown in Fig. 6. A fit to all of the data points gives a slope of -0.7 . If we exclude the inner data point, which lies at the radius expected for the GC system core size (see Forbes *et al.* 1996), the slope steepens slightly to -0.8 . Even at -0.8 , the surface density slope is, to our knowledge, the flattest measured for GC systems (Kissler–Patig 1996). We have not made any correction for background galaxy contamination. We note that Haynes & Giovanelli (1991) have studied the region around the NGC 5846 group. They find both nearby and distant galaxies to the north and west of NGC 5846. Our data do not cover the west of NGC 5846 but do include a northern pointing. Indeed there appears to be an enhancement of faint galaxies in CCDs 2 and 3 in the north pointing. Our selection process, after applying the size and color cuts, excludes the obvious resolved galaxies. It is possible that compact background galaxies remain in our object list in the northern pointing.

However, the surface density in the northern pointing is similar to that of the southern pointing at a given galactocentric radius, including that background galaxy contamination, if any, is negligibly small. The WFPC2 geometry makes it difficult to measure the galaxy starlight slope, but we estimate it to be ~ -1.5 . Thus the GC system appears to have a much flatter surface density slope and is more extended than the galaxy light. This situation is common for elliptical galaxies (e.g. Grillmair *et al.* 1994). Since the galaxy light falls off faster with radius than the density of GCs, we would expect the local S_N value (i.e. the number of GCs normalized by the galaxy light out to that radius) to increase with radius. This is indeed seen in Fig. 7, in which the local S_N increases from ~ 0.2 at 1 kpc to 2 at 12 kpc. We expect the S_N value to increase smoothly to the global value of 4.3 ± 1.1 at a radius of 50 kpc. The total number of GCs out to 50 kpc is estimated to be 4670 ± 1270 , which is roughly twice the estimate of Harris & van den Bergh (1981) from photographic plates. We conclude that NGC 5846 has a much lower specific frequency than other dominant ellipticals in rich clusters but is similar to dominant ellipticals in groups (e.g. Bridges & Hanes 1994).

The azimuthal distribution of GCs is generally consistent with a spherical distribution, which is similar to the underlying galaxy light i.e., type E0–1. However, there is evidence for a slight enhancement of counts around position angle 20° and a deficit at 100° . If this effect is real, the GCs appear to be aligned closer to the galaxy’s minor axis than its major axis (P.A. $\sim 100^\circ$). The nearest galaxy to NGC 5846 is NGC 5846A, which lies to the south (P.A. $\sim 190^\circ$).

4.4. Implications for Globular Cluster Formation

One of main results from this study is that NGC 5846 has a bimodal color and, by inference, metallicity distribution. A handful of other galaxies (usually having high luminosity and high S_N) also reveal bimodality. This indicates that there has been more than one epoch of GC formation in these galaxies. A bimodal metallicity distribution is a prediction of the Ashman & Zepf (1992) merger model. In this model the blue GCs are thought to be the metal-poor population from the progenitor galaxies and the red GCs are metal-rich ones formed in the merging process. The red GCs are expected to be more centrally concentrated than the blue GCs (which is hinted at in NGC 5846). However, this model has some difficulty in explaining other features. For example, to produce a luminosity of $M_V = -22.6$ the merging of $\sim 10 L^*$ spirals would be required. It is difficult to imagine a clear bimodal GC distribution emerging from such a history. The presence of filamentary dust in the central regions suggests a recent encounter with a gas-rich galaxy. The short dynamical times in this region ($\leq 10^8$ yrs) and the fact that the GCs appear to be over 1 Gyr old suggest that GCs did not form from this event.

As mentioned in the introduction, M87 and NGC 5846 have a similar X-ray luminosity and cooling flow rate and yet M87 has about three times as many GCs per unit starlight as NGC 5846. These results support the view of Bridges *et al.* (1996) that the bulk of GCs did *not* form in a cooling flow. Other mechanisms (such as a two-phase collapse or the accretion of external GCs) should be considered to explain the GC bimodality in NGC 5846. We note that NGC 5846A, a compact E2 galaxy

with $M_V \sim -18.5$, lies ~ 6 kpc south of NGC 5846. The GCs of NGC 5846A may have contributed to those of NGC 5846 via tidal stripping and may contribute even more if the whole galaxy is eventually accreted. Unfortunately, NGC 5846A is not covered by our WFPC2 images.

5. Conclusions

Using deep multi-filter WFPC2 images, we discuss the color and spatial distributions of the globular cluster system in NGC 5846. We find a bimodal color distribution with peaks at $V-I = 0.96$ and 1.17 in all three WFPC2 pointings. These roughly correspond to metallicities of $[\text{Fe}/\text{H}] = -1.2$ and -0.2 respectively. Such a bimodal distribution suggests that at least formation episodes have contributed to the GC system. The red (metal-rich) population may be more centrally concentrated than the blue (metal-poor) population. The radial metallicity gradient is $\Delta[\text{Fe}/\text{H}]/\Delta\log R$ (arcsec) = -0.13 ± 0.03 . Both subpopulations have the same luminosity functions, within an uncertainty of 0.3 mag. Thus we find no evidence for a luminosity-metallicity relation within an individual galaxy's globular cluster system. Previous work on the Milky Way and M31 reached a similar conclusion (Huchra, Brodie & Kent 1991). For a constant mass-to-light ratio, the lack of a mass-metallicity relation for globular clusters, allows several formation models to be ruled out (ones in which a metallicity cooling criterion imprints a characteristic mass).

The surface density of GCs falls off much more slowly with radius than the galaxy light. The best-fit power law gives a slope of ~ -0.75 which appears to be the flattest globular cluster systems known. The globular clusters

appear to be better aligned with the galaxy's minor axis than its major axis, although this result is of marginal significance. We find that the specific frequency increases steadily with radius in the inner regions and reaches a global value of 4.3 ± 1.1 at 50 kpc. Thus NGC 5846 has a much lower specific frequency than other dominant ellipticals in clusters but is similar to dominant ellipticals in groups.

The galaxy isophotes deviate from pure ellipses and become slightly boxy (extra light at 45° to the major axis) in the central regions, perhaps due to the filamentary dust. The dust is probably the result of a past merger or accretion of a gas-rich galaxy and provides the fuel for the compact radio core. We have searched for proto-globular clusters associated with the dust (and gas) and find none.

Acknowledgments

We thank C. Grillmair, M. Kissler-Patig and M. Rabban for helpful discussions. We also thank the referee, J. Secker, for his comments. This research was funded by the HST grant GO-05920.01-94A

References

- Ashman, K. M., & Zepf, S. E. 1992, *ApJ*, 384, 50
- Ashman, K. M., Conti, A., & Zepf, S. E. 1995, *AJ*, 110, 1164
- Bender, R., Burstein, D., & Faber, S. M. 1992, *ApJ*, 399, 462
- Biermann, P. L., Kronberg, P. P., & Schmutzler, T. 1989, *A & A*, 208, 22
- Bridges, T. J., & Hanes, D. A. 1994, *ApJ*, 431, 625
- Bridges, T. J., Hanes, D. A., & Harris, W. E. 1991, *AJ*, 101, 469
- Bridges, T. J., Carter, D., Harris, W. E., & Pritchett, C. J. 1996, *MNRAS*, in press
- Bruzual, G., & Charlot, S. 1996, in preparation
- Carollo, C. M., Franx, M., Illingworth, G. D., & Forbes, D. A. 1996, *ApJ*, submitted
- Couture, J., Harris, W. E., & Allwright, J. W. B., 1990, *ApJS*, 73, 671
- Elson, R. A. W., & Santiago, B. X. 1996, *MNRAS*, 280, 971
- Faber, S. M., *et al.* 1989, *ApJS*, 69, 763
- Fabian, A. C., Nulsen, P. E. J., & Canizares, C. R. 1984, *Nature*, 310, 733
- Fisher, D., Franx, M., & Illingworth, G. D. 1995, *ApJ*, 448, 119
- Forbes, D. A., & Thomson, R. C. 1992, *MNRAS*, 254, 723
- Forbes, D. A., Franx, M., & Illingworth, G. D. 1995, *AJ*, 109, 1988
- Forbes, D. A., Brodie, J. P., & Huchra, J. 1996, *AJ* in press
- Forbes, D. A., Grillmair, C. J., & Brodie, J. P. 1996, in preparation
- Forbes, D. A., Franx, M., Illingworth, G. D., & Carollo, C. M. 1996, *ApJ*, in press
- Forte, J. C., Martinez, R. E., & Muzzio, J. C. 1982, *AJ*, 87, 1465
- Goudfrooij, P., & Trinchieri, G. 1996, in preparation
- Geisler, D., Lee, M. G., & Kim, E. 1996, *AJ*, in press
- Grillmair, C. *et al.* 1994, *AJ*, 108, 102
- Harris, W. E., & van den Bergh, S. 1981, *AJ*, 86, 1627
- Haynes, M. P., & Giovanelli, R. 1991, *AJ*, 102, 841
- Holtzman, J., *et al.* 1992, *AJ*, 103, 691
- Holtzman, J., *et al.* 1996, *AJ*, 112, 416
- Huchra, J., Brodie, J. P., & Kent, S. 1991, *ApJ*, 370, 495
- Kissler-Patig, M., 1996, *A & A*, in press
- Lauer, T., *et al.* 1995, *AJ*, 110, 2622
- Longo, G., & de Vaucouleurs, A. 1983, *A General Catalogue of Photometric Magnitudes and Colors in the UBV system (University of Texas, Austin)*
- Mollenhoff, C., Hummel, E., & Bender, R. 1992, *A & A*, 255, 35
- McLaughlin, D. E., Harris, W. E., & Hanes, D. A. 1993, *ApJ*, 409, L45
- McLaughlin, D. E., Secker, J., Harris, W. E., & Geisler, D. 1995, *AJ*, 109, 1033
- Murali, C., & Weinberg, M. D. 1996, *MNRAS*, in press
- Searle, L., & Zinn, R. 1978, *ApJ*, 437, 214
- Secker, J. 1996, *ApJL*, 469, 81
- Secker, J., & Harris, W. E. 1993, *AJ*, 105, 1358 (SH93)
- Stetson, P. B., 1987, *PASP*, 99, 191
- West, M. J., Cote, P., Jones, C., Forman, W., & Marzke, R. O. 1995, *ApJ*, 453, L77
- Whitmore, B. C., Schweizer, F., Leitherer, C., Borne, K., & Robert, C. 1993, *AJ*, 106, 1354
- Whitmore, B. C., & Schweizer, F. 1995, *AJ*, 109, 960
- Whitmore, B. C., Sparks, W. B., Lucas, R. A., Macchetto, F. D., & Biretta, J. A. 1995, *ApJ*, 454, L73
- Zepf, S. E., Ashman, K. M., & Geisler, D. 1995, *ApJ*, 443, 570

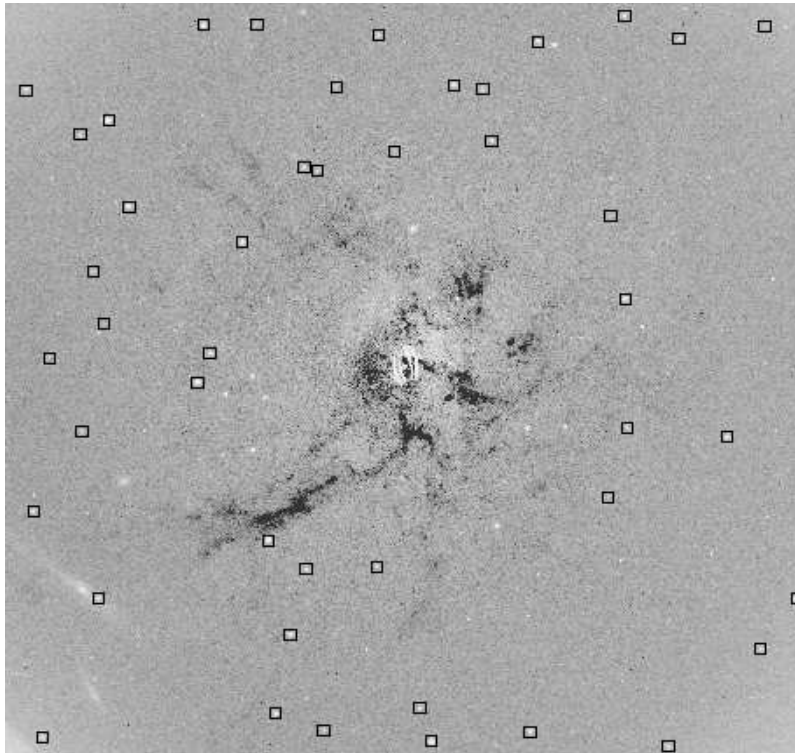


Fig. 1.— Grey scale WFPC2 image of the PC CCD (about $30'' \times 30''$ area) of the central region of NGC 5846. The automatically selected globular clusters beyond $7''$ (1 kpc) from the galaxy center are indicated by black squares. Several radial dust filaments can be seen reaching into the nucleus.

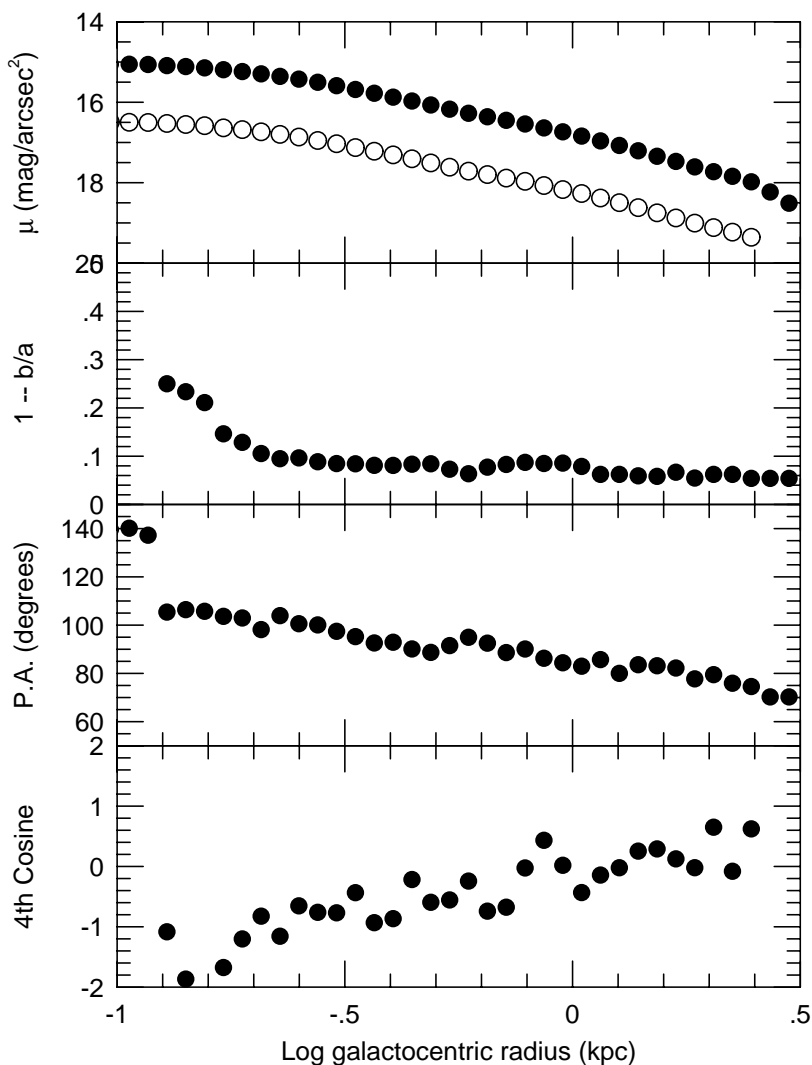


Fig. 2.— Galaxy properties within $20''$ (3 kpc). We show surface brightness, ellipticity, position angle and the 4th cosine term deviations from a pure ellipse. The I band data are represented by filled circles and the V band surface brightness data by open circles. In the central regions, NGC 5846 has near constant V–I color and ellipticity. The position angle changes from 70° to $\sim 100^\circ$ near the nucleus, and 4th cosine term becomes more boxy.

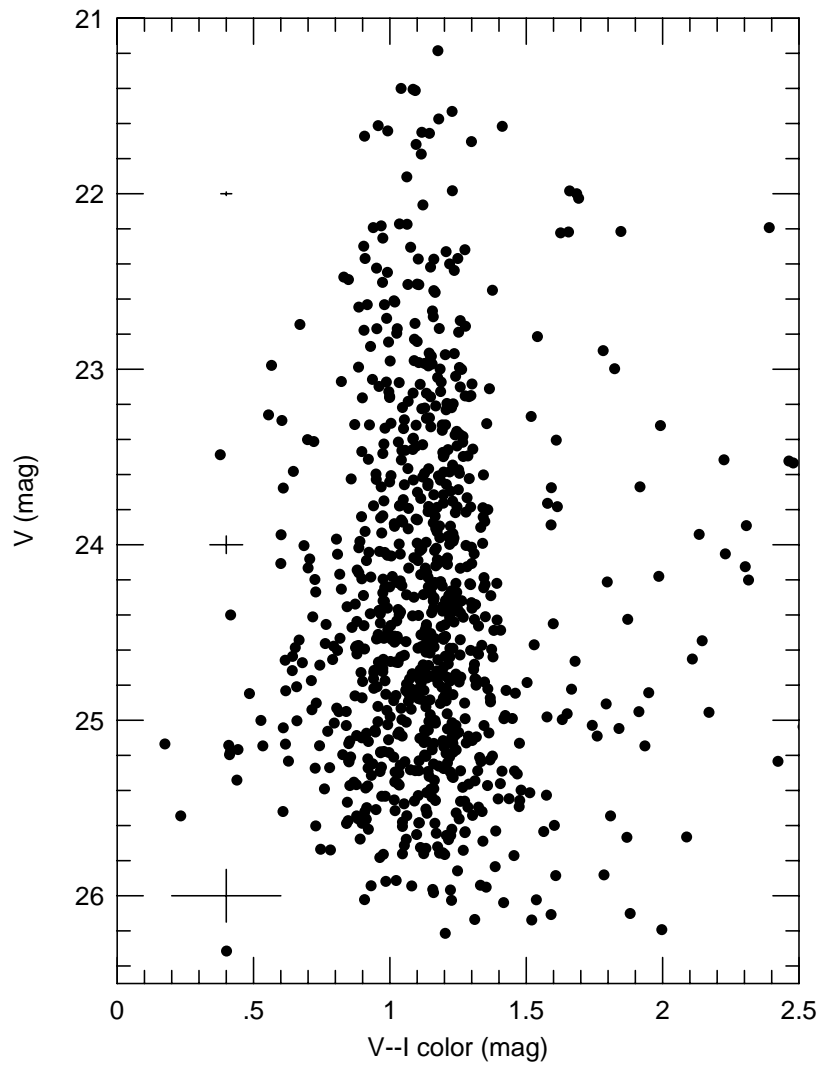


Fig. 3.— Color-magnitude diagram for a sample of 837 globular clusters around NGC 5846. Typical error bars are shown on the left. The globular cluster color is roughly constant with magnitude.

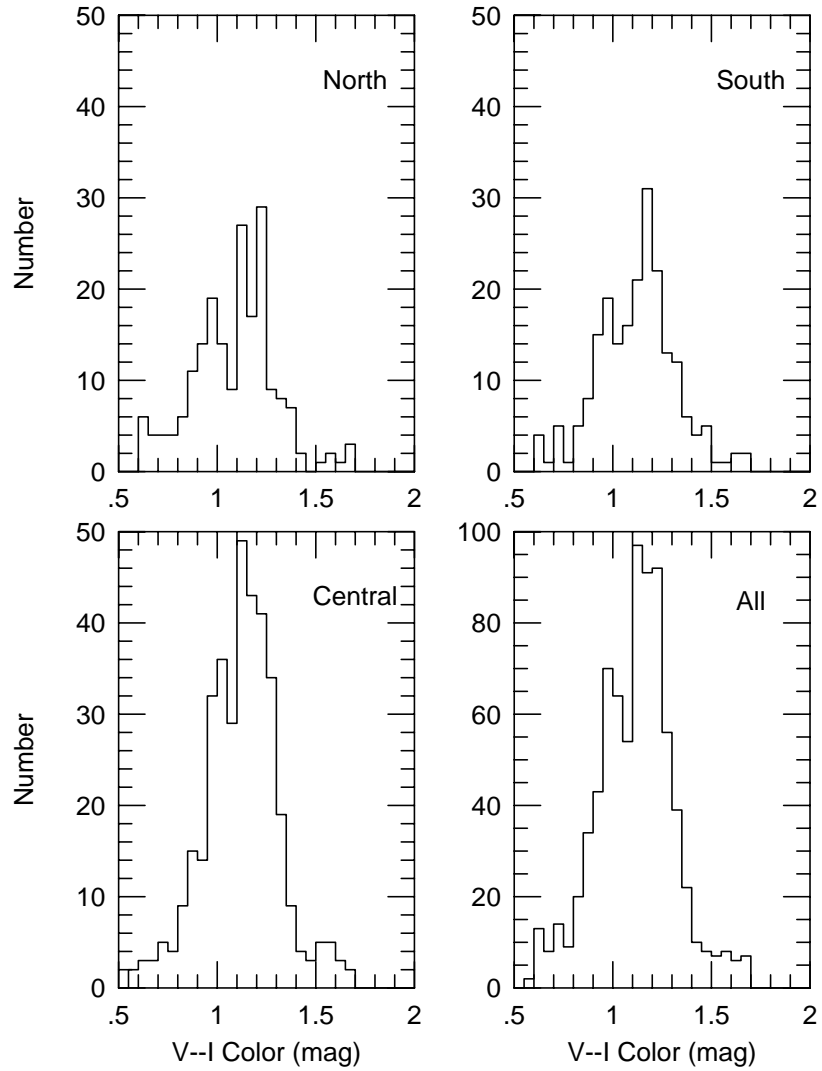


Fig. 4.— Histograms of globular cluster V-I colors (within 3σ of the mean color). The four panels show data from the north, south and central pointings, along with the combined sample. A clear bimodal color distribution can be seen.

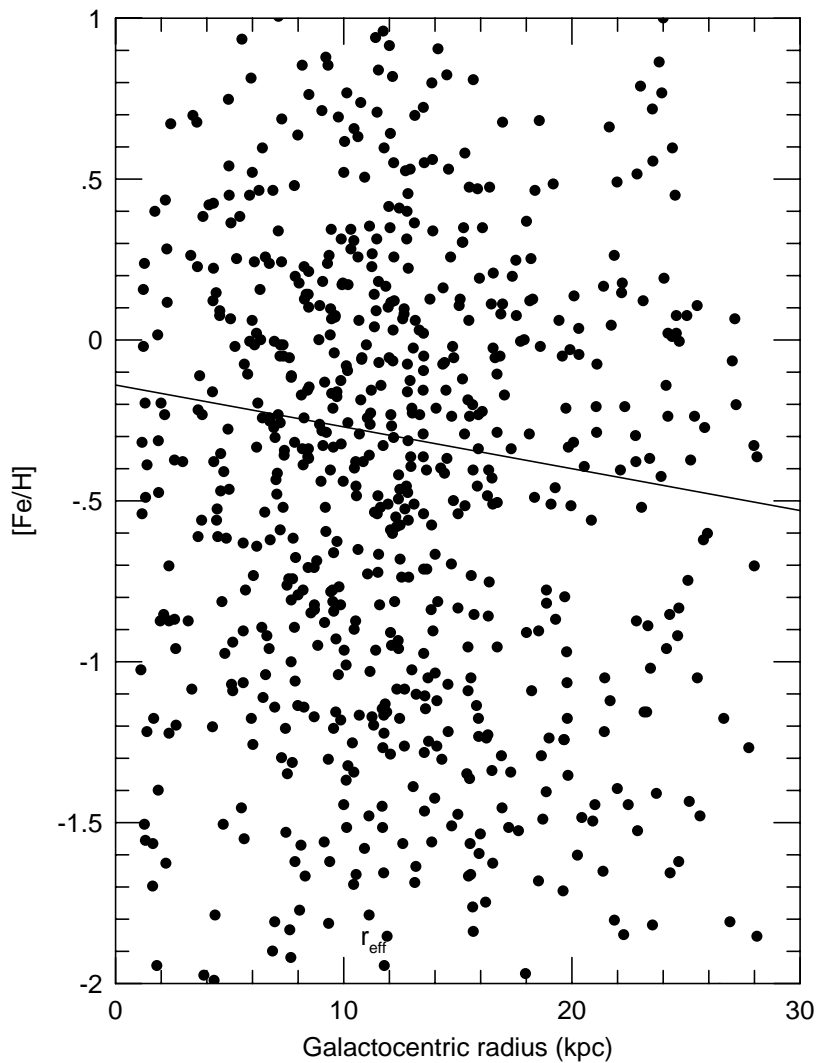


Fig. 5.— Radial variation of globular cluster metallicity. The solid line represents a weighted fit to the data. There is a shallow metallicity gradient. The effective radius of the galaxy (r_{eff}) is also indicated. The typical random error of each data point is ± 0.25 .

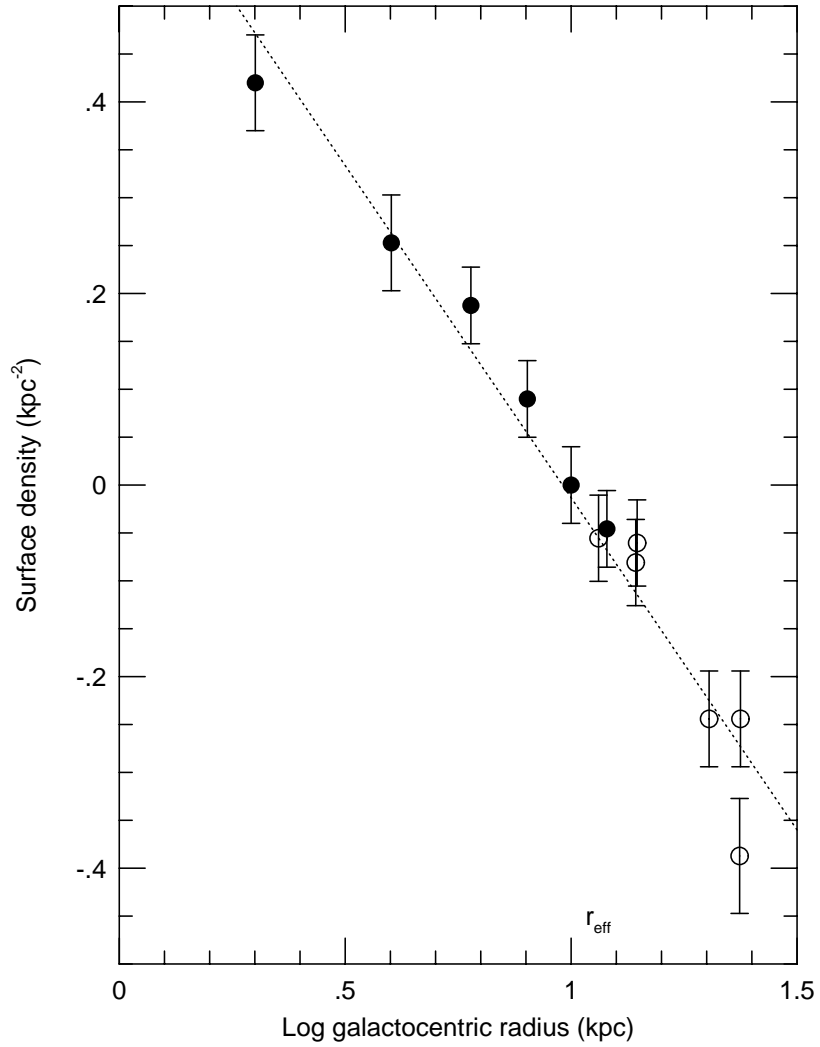


Fig. 6.— Surface density profile of globular clusters. The surface density has been calculated using two different methods (see text for details) which are represented by open and filled circles. Error bars represent Poisson statistics. The dashed line is a best fit to all data points, which gives a slope of -0.7 .

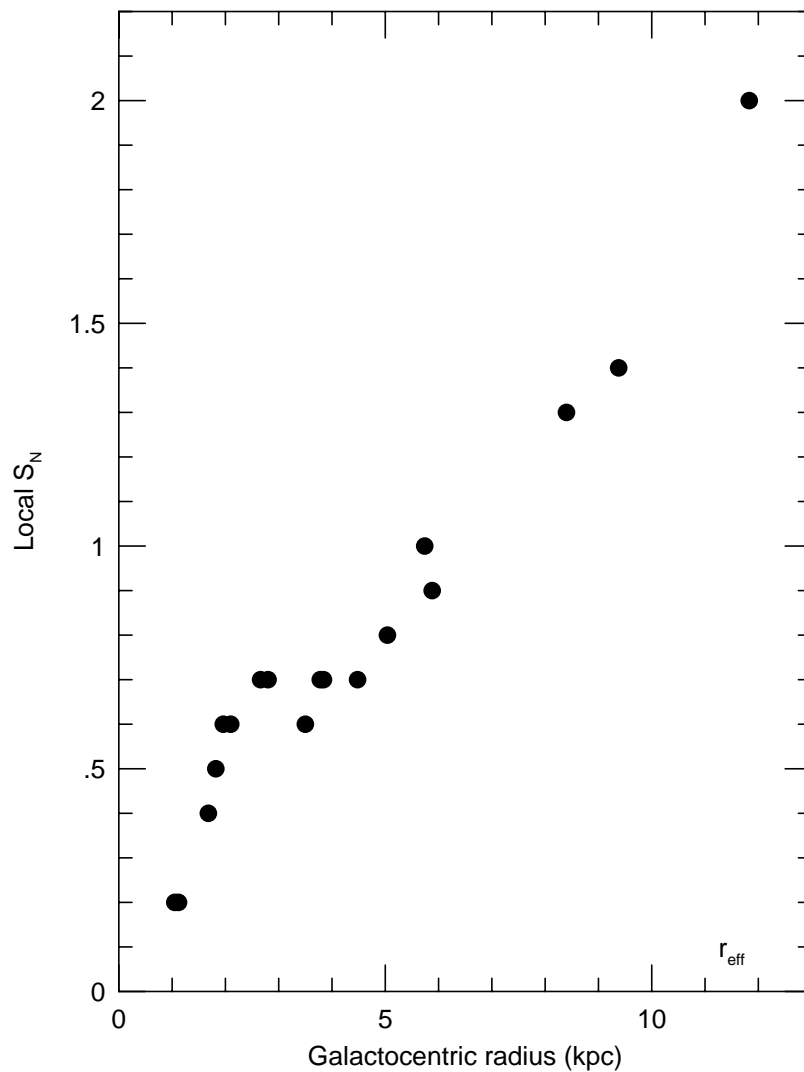


Fig. 7.— Radial variation of local specific frequency. The local specific frequency is the number of globular clusters normalized by the integrated galaxy light at each radius. The local S_N increases with distance from the galaxy center, reaching a global value of 4.3 at 50 kpc.

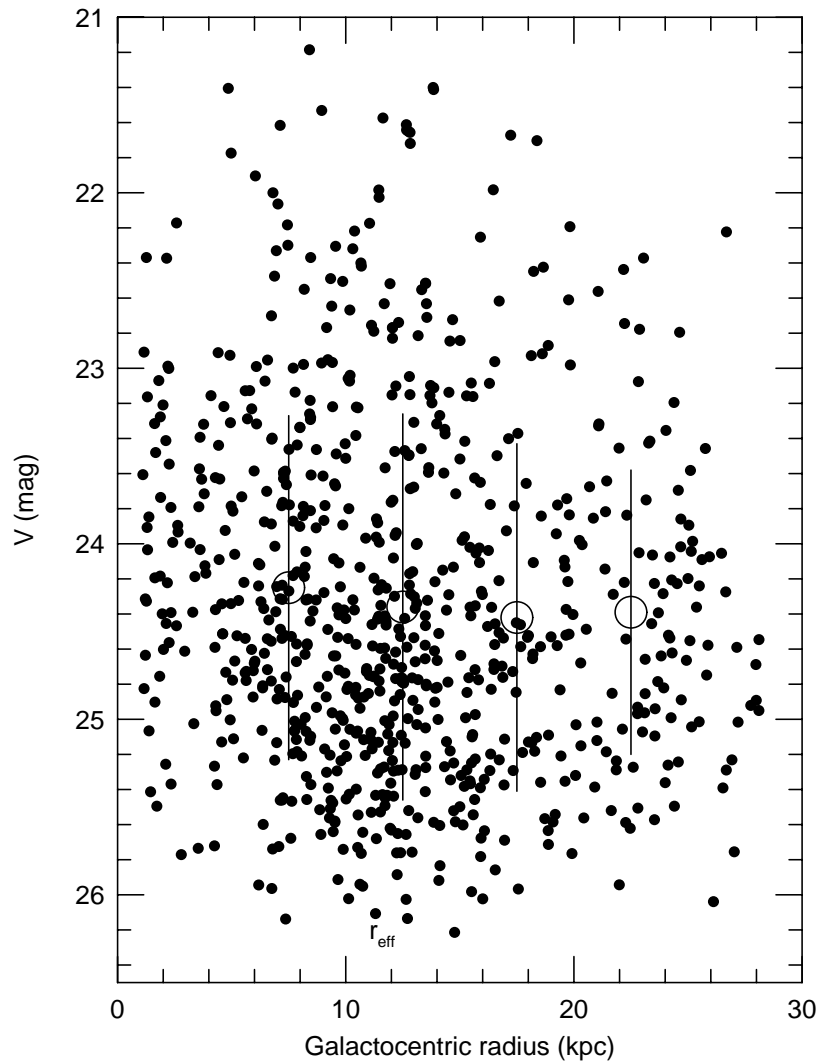


Fig. 8.— Radial variation of V magnitude. The mean magnitude in 4 bins is indicated along with the rms scatter. There is little or no magnitude gradient beyond the central PC CCD (~ 2.5 kpc), which has a slightly brighter detection limit.

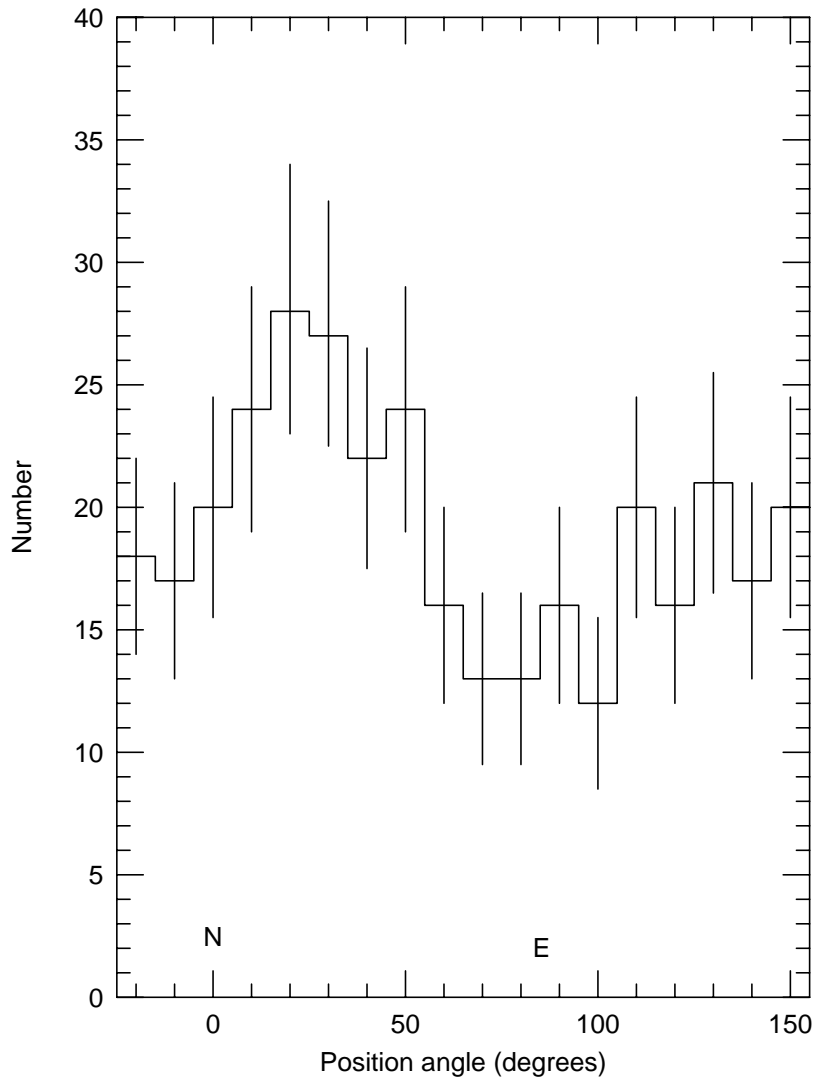


Fig. 9.— Histogram of globular cluster position angle. Error bars represent Poisson statistics. North and East are indicated. The galaxy major axis lies at $\sim 100''$. The globular clusters reveal a slight enhancement at $\sim 20^\circ$ but otherwise appear consistent with a spherical distribution.

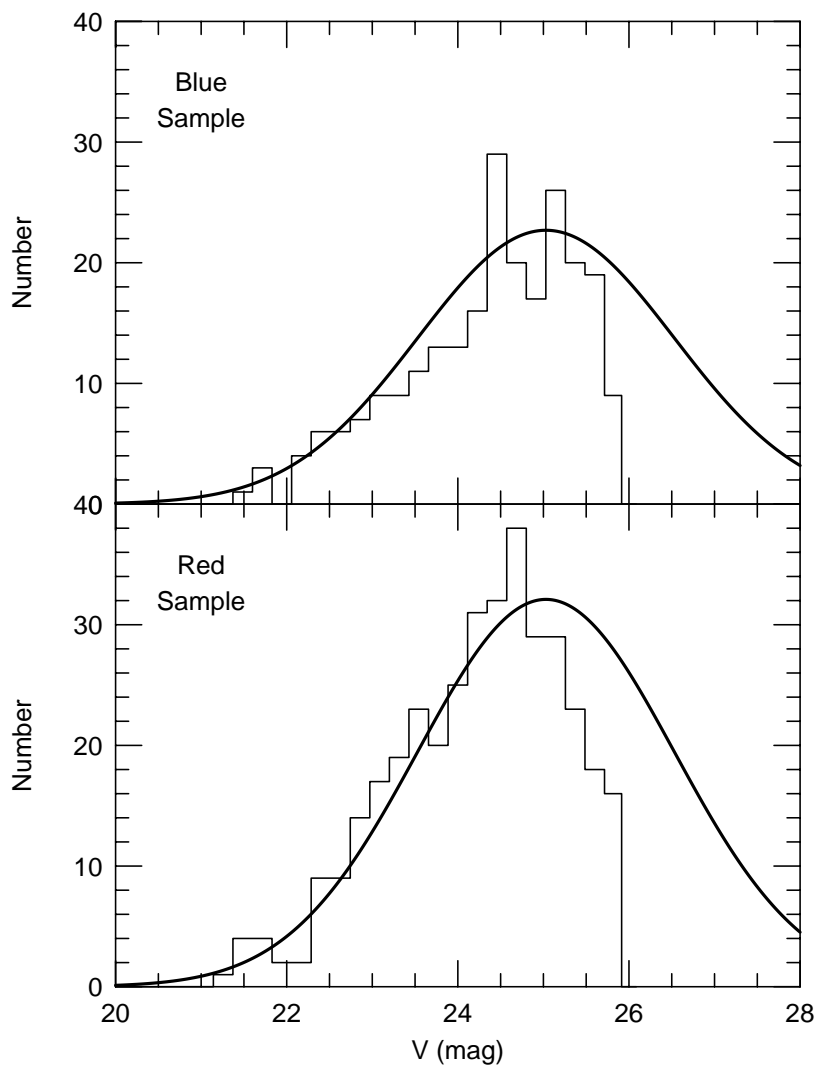


Fig. 10.— Globular cluster luminosity functions for the red and blue samples. A Gaussian profile with a turnover magnitude appropriate for the full sample has been superposed and arbitrarily scaled in the vertical direction.

